Count	CpG Site	UCSC Gene	UCSC Region	Relation to Island	Methylation (Cultured Fibroblasts)	Gene Expression (Culture Fibroblasts)
1	cg12432010	IQSEC3	1stExon	Island	Hyper (10%)	Undetected
2	**cg25391162**	**FOXD4**	**1stExon**	**Island**	**Hyper (15%)**	**Upregulated (333%)**
3	cg01503065	DCHS2	1stExon	Island	Hyper (9%)	Not Significant
4	cg00059225	GLRA1	1stExon;5'UTR	Island	Hyper (14%)	Undetected
5	cg06665453	TSEN54;LLGL2	3'UTR;TSS1500	N_Shore	Hyper (18%)	Not Signifcant;Undetected
6	cg00741624	KIAA1409	5'UTR	Island	Hyper (8%)	Undetected
7	cg25032595	CLDN10	5'UTR;1stExon;Body	Island	Hyper (27%)	Not Significant
8	**cg17593472**	**FGF1**	**5'UTR;1stExon;Body;TSS200**	**OpenSea**	**Hyper (21%)**	**Upregulated (361%)**
9	cg15341124	DIO3;MIR1247	5'UTR;1stExon;TSS1500	Island	Hyper (7%)	Undetected;Undetected
10	cg00003345	CASZ1	5'UTR	OpenSea	Hyper (21%)	Undetected
11	cg03615565	FAM65A	Body	Island	Hyper (34%)	Not Significant
12	cg07544187	CILP2	Body	Island	Hyper (20%)	Not Significant
13	cg13654588	PRLHR	Body	Island	Hyper (16%)	Undetected
14	cg15243034	USP35	Body	Island	Hyper (44%)	Not Significant
15	cg00481951	SST	Body	N_Shore	Hyper (6%)	Undetected
16	**cg07022048**	**KRT7**	**Body**	**N_Shore**	**Hypo (-22%)**	**Upregulated (250%)**
17	cg04999352	RARRES3	Body	OpenSea	Hyper (8%)	Not Significant
18	cg22108374	CCDC33	Body	OpenSea	Hyper (46%)	Undetected
19	cg27401724	ACBD4	Body	S_Shelf	Hypo (-19%)	Not Significant
20	cg26470501	BCL3	Body	S_Shore	Hyper (21%)	Not Significant
21	cg23527621	ECE2;CAMK2N2	Body;3'UTR	Island	Hypo (-15%)	Not Significant;Not Significant
22	cg11071401	CACNA1G	TSS1500	Island	Hyper (37%)	Undetected
23	**cg16867657**	**ELOVL2**	**TSS1500**	**Island**	Hyper (22%)	**Downregulated (-83%)**
24	**cg22809047**	**RPL31**	**TSS1500**	**Island**	Hypo (-31%)	**Downregulated (-22%)**
25	cg27320127	KCNK12	TSS1500	Island	Hyper (5%)	Undetected
26	cg24168221	CST9	TSS1500	OpenSea	Hyper (38%)	Undetected
27	**cg25410668**	**RPA2**	**TSS1500**	**S_Shore**	Hyper (26%)	**Upregulated (35%)**
28	**cg22454769**	**FHL2**	**TSS200;5'UTR**	**Island**	Hyper (29%)	**Upregulated (155%)**
29	cg01490733	Unclassified	Unclassified	Island	Hyper (19%)	Unclassified
30	cg15168727	Unclassified	Unclassified	Island	Hyper (17%)	Unclassified
31	cg19821713	Unclassified	Unclassified	Island	Hyper (23%)	Unclassified
32	cg16008966	Unclassified	Unclassified	OpenSea	Hypo (-22%)	Unclassified
33	cg11793449	Unclassified	Unclassified	S_Shelf	Hyper (11%)	Unclassified
34	cg17110586	Unclassified	Unclassified	S_Shelf	Hyper (6%)	Unclassified
35	cg06931612	Unclassified	Unclassified	S_Shore	Hyper (14%)	Unclassified

Supplemental Table S1. Overlapping CpGs across in vivo in vitro whole blood and fibroblast datasets

Table of descriptive information of 35 overlapping age-associated sites between fibroblast and whole blood In Vivo and In Vitro datasets. Bolded CpG Sites indicate CpG sites on genes that are differentially expressed by >0.2 fold with age.

Supplemental Figure S1

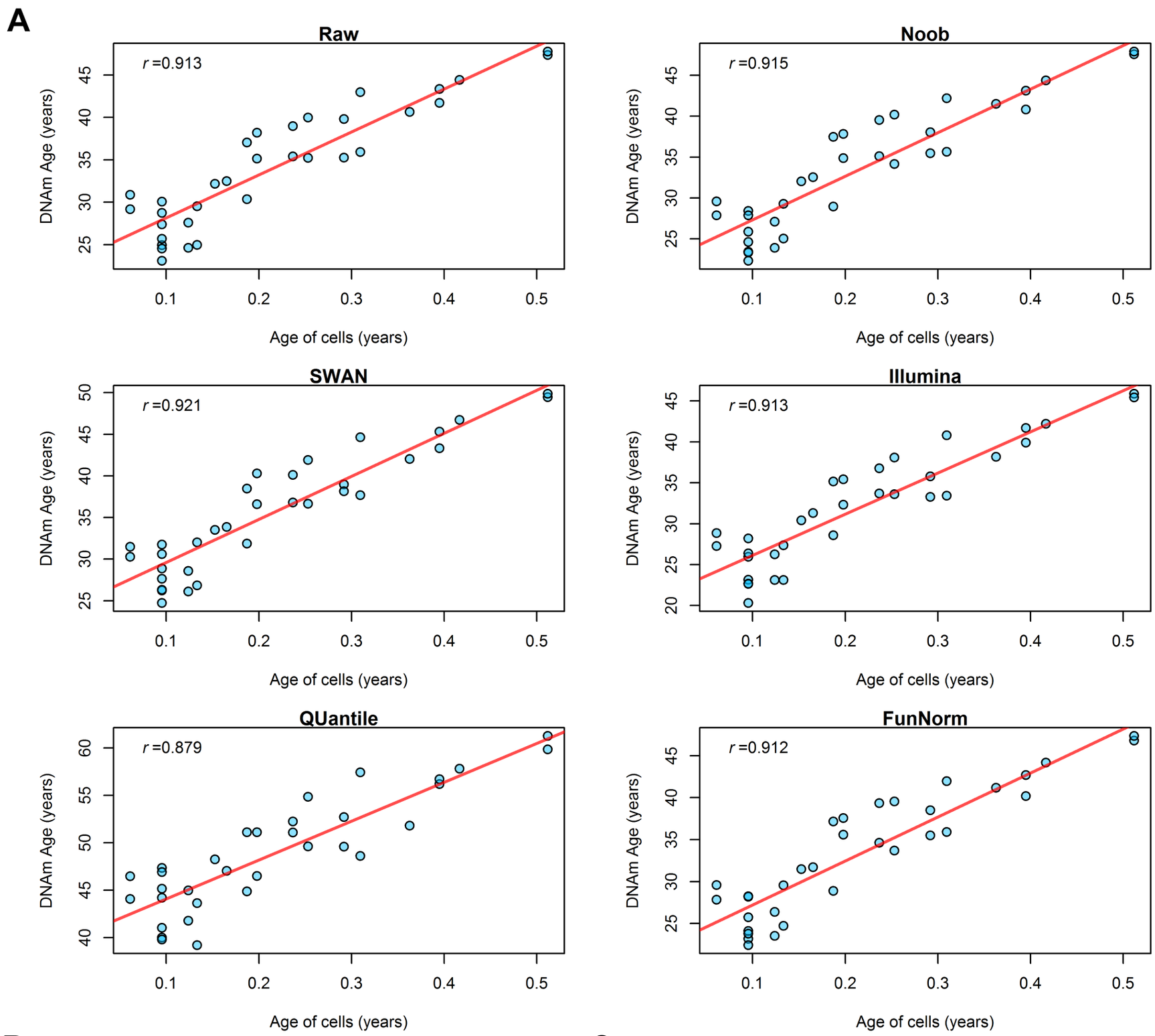

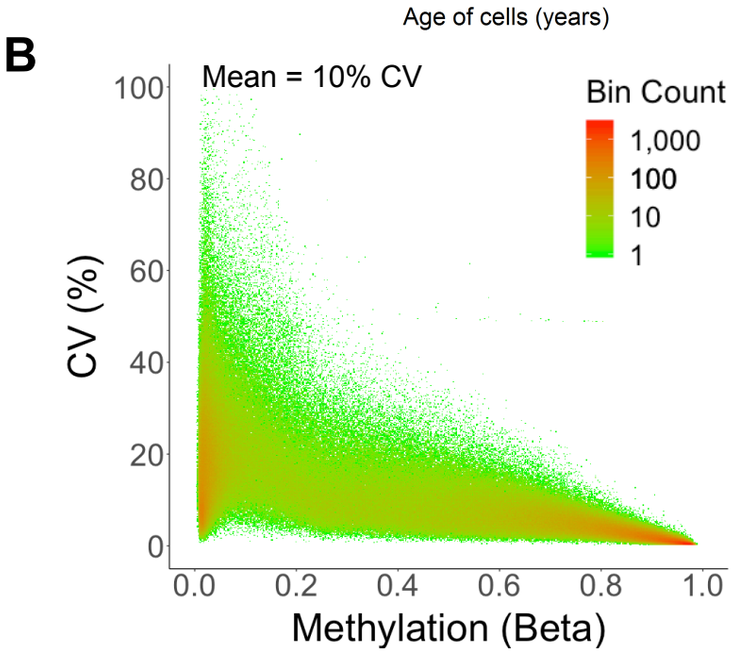

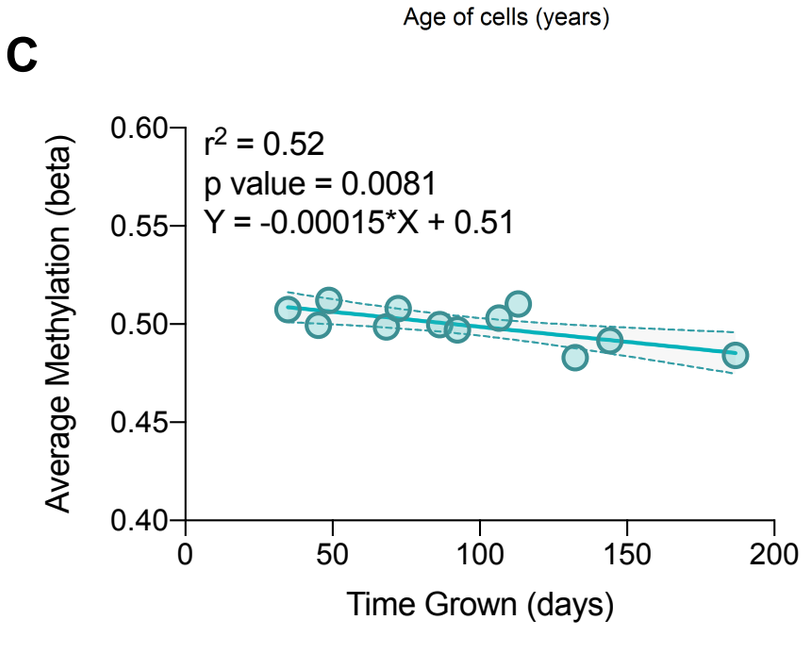

S1. Comparison of EPIC array normalization methods and quantification of technical variability.

(**A**) Comparisons of six normalization methods and their effect on predicted DNAmAge (PanTissue clock) regressed on chronological age. The red line indicates the linear fit line. This data demonstrates minimal effect of normalization methods on predicted DNAm age. (**B**) The calculated coefficient of variation (C.V.) measured from six technical replicates (45-day timepoint, normal glucose) distributed across different EPIC arrays. Measurement error is higher for sites with low methylation levels (beta values). Each datapoint is the C.V. for a single CpG. Color scheme indicates density of overlapping CpGs (log scale) on the scatterplot. (**C**) Linear regression of the average DNAm levels across all CpGs sites for each timepoint studied across the cellular lifespan. The global slope reflects a 5.5% decrease in global DNAm per calendar year.

Supplemental Figure S2

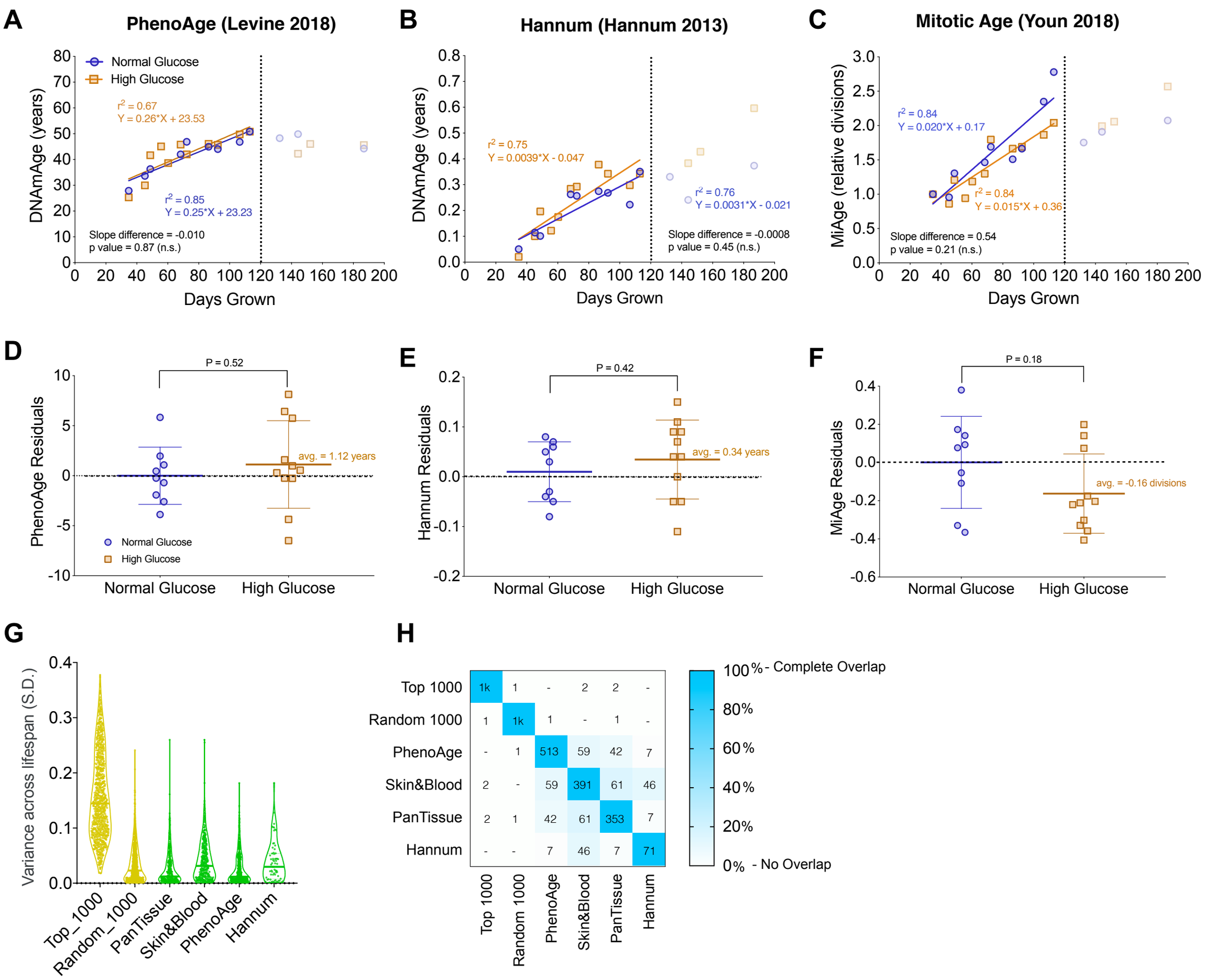

S2. The PhenoAge clock, Hannum clock, and MiAge calculator track cellular aging in early- and mid-life.

(**A**) The PhenoAge Clock (Levine et al., 2018) trained on blood to predict clinical age related phenotypic characteristics; (**B**) The Hannum Clock trained on blood to predict chronological age; (**C**) DNA methylation-based estimation of mitotic age trained on human tumors and blood to predict the number of cell divisions or population doublings, predicted divisions are shown relative to youngest 35 day timepoint. Shown are correlations of chronological age (days in culture) and predicted DNAmAge with each clock, indicating linear increase in DNAmAge for the early- and mid-life periods, but not beyond the point of transition towards replicative senescence (dotted line, 120 days). Results for both normal (5.5 mM) and high (25 mM) glucose are shown and do not differ in their rate of aging. (**D-F**) Box plots of residuals from the regression of actual and predicted age for normal and high glucose cells across entire lifespan. Non-parametric unpaired Mann-Whitney test. (**G**) Average age-related variation among the CpGs that compose the various DNAm clocks and the top 1,000 most significant sites in fibroblast experiments. This reveals that clock CpGs exhibit small to moderate effect sizes across the lifespan compared to the top 1,000 most significant sites in fibroblasts. All clocks show strong predictive power across the cellular lifespan despite the small effect sizes of each CpG, highlighting the added value of computationally integrating multiple CpG sites in DNAm clocks. (**H**) Proportion of overlap between different DNAmAge clocks, the top 1,000 most significant CpGs in fibroblasts, and 1,000 CpGs randomly selected from the EPIC array. Shown in each box is the number of overlapping CpGs between each group, dash indicates 0 overlapping sites.

Supplemental Figure S3

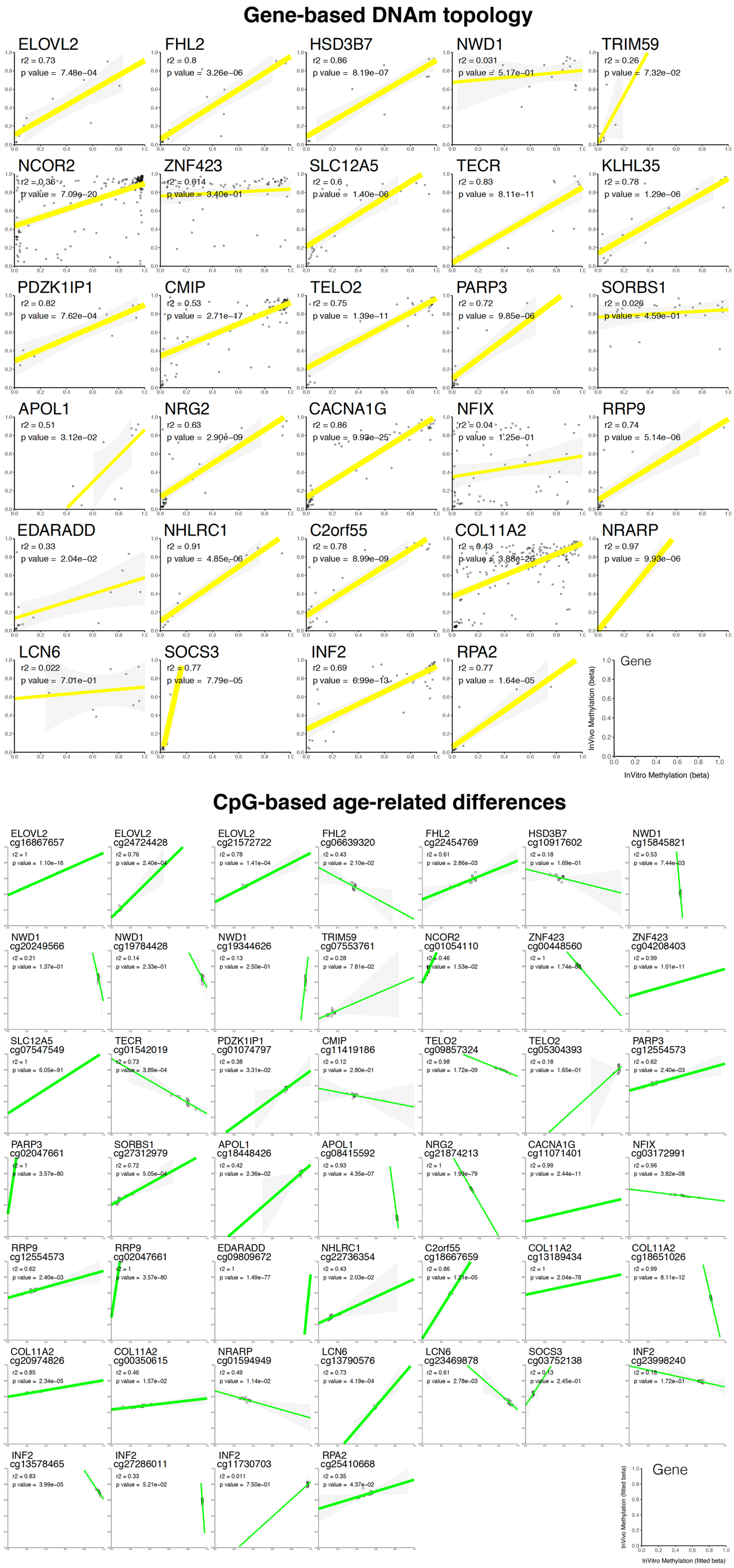

Figure S3. ***DNAm gene topology and age-related CpG differences are generally conserved between human blood and cultured fibroblasts.***

Higher magnification version of the Figure 3E-F, including correlation coefficients and p values. Only regressions with positive correlations are shown as significant (thick regression line).

Supplemental Figure S4

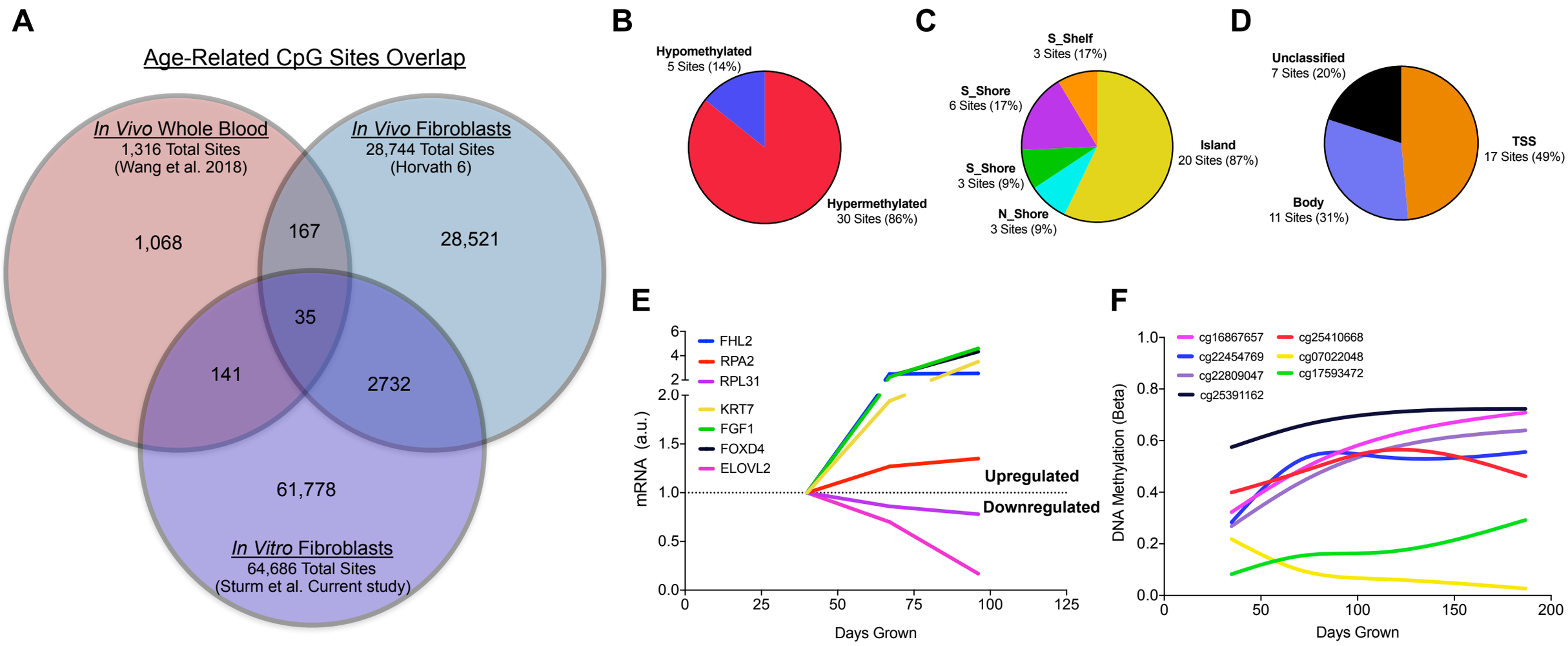

Figure S4. Overlap of age-related DNA methylation changes between in vitro and in vivo fibroblasts and whole blood.

(**A**) Overlap of statistically significant (Bonferroni-corrected) age-associated sites among different *in vivo* (human blood) and *in vitro* (cultured fibroblasts) studies. Note that there are more significant CpGs in cultured cells systems compared to human studies, likely due to the controlled experimental conditions *in vitro*. Only 35 CpGs overlap between the three datasets. (**B-D**) Proportions of the 35 replicated age-associated CpGs that undergo hyper- or hypo-methylation, (**B**) their position relative to CpG islands, and (**C**) and gene regions. See Supplemental Table S1 for complete annotation. (**E**) Of the 35 overlapping CpGs, 7 mapped to a gene that was differentially expressed (>0.2 fold change in transcript levels) measured by RNAseq. (**F**) Color coded DNAm levels for the CpG that map to each gene shown in (E).

Supplemental Figure S5

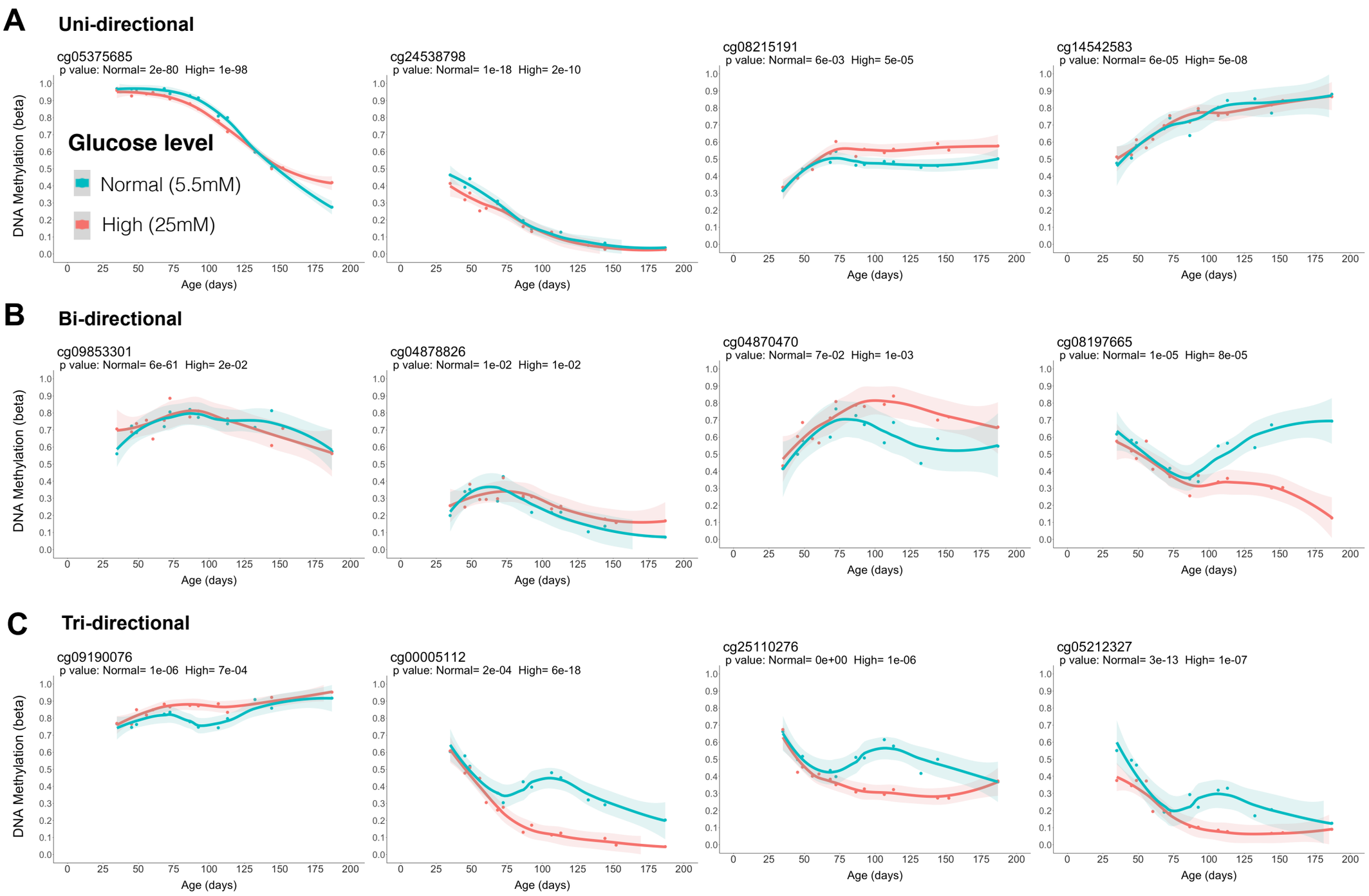

S5. Exploratory analysis of non-monotone CpG trajectories.

(**A**) DNAm kinetics across the cellular lifespan for CpG sites exhibiting monotone, (**B**) bi-tone, and (**C**) tri-tone trajectories. Each CpG is shown for cells aging under either normal and high glucose. Non-monotone sites were handpicked form a list of GAM-fitted sites with up to 9 DoF.

Supplemental Figure S6 - Part 1

Supplemental Figure S6 - Part 2

Gene | **Methylation Topology** | **Sig. CpG Sites** | **RNAseq** (Cultured Fibroblasts)

ZNF423
13th Percentile
GeneCard

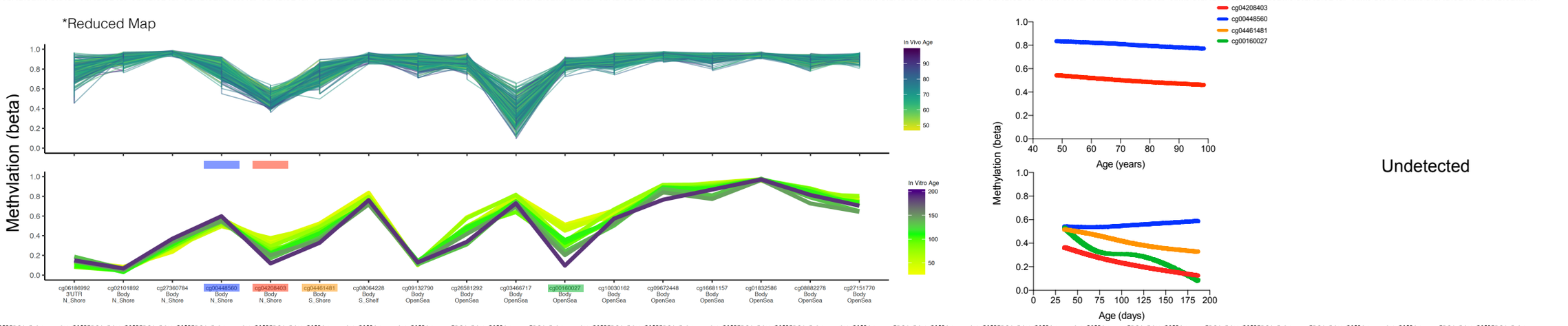

Undetected

SLC12A5
Unexpressed
GeneCard

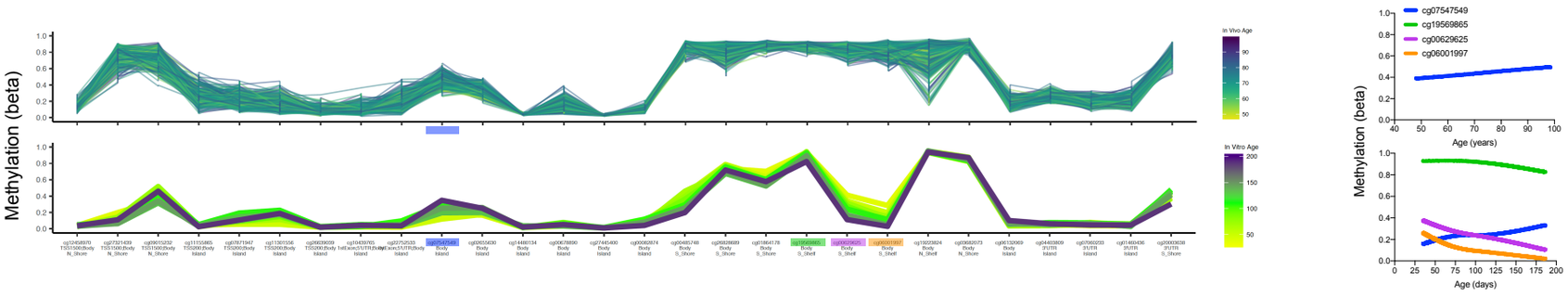

Undetected

TECR
80th Percentile
GeneCard

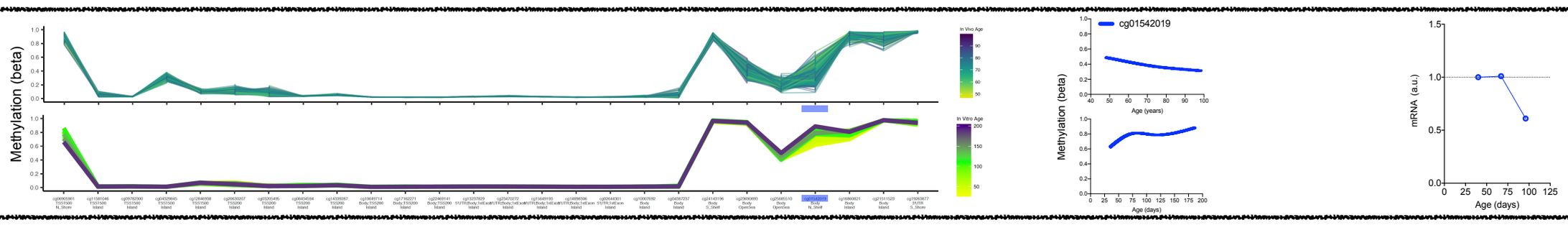

KLHL35
56th Percentile
GeneCard

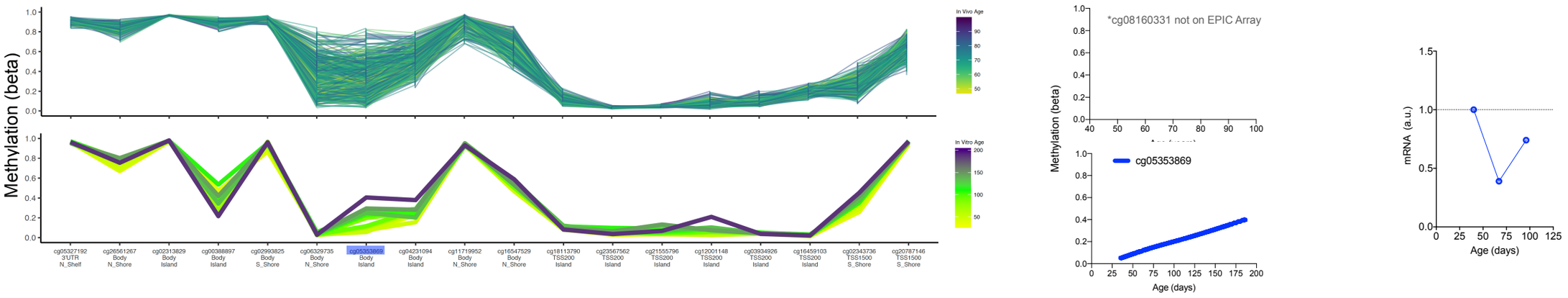

PDZK1IP1
21st Percentile
GeneCard

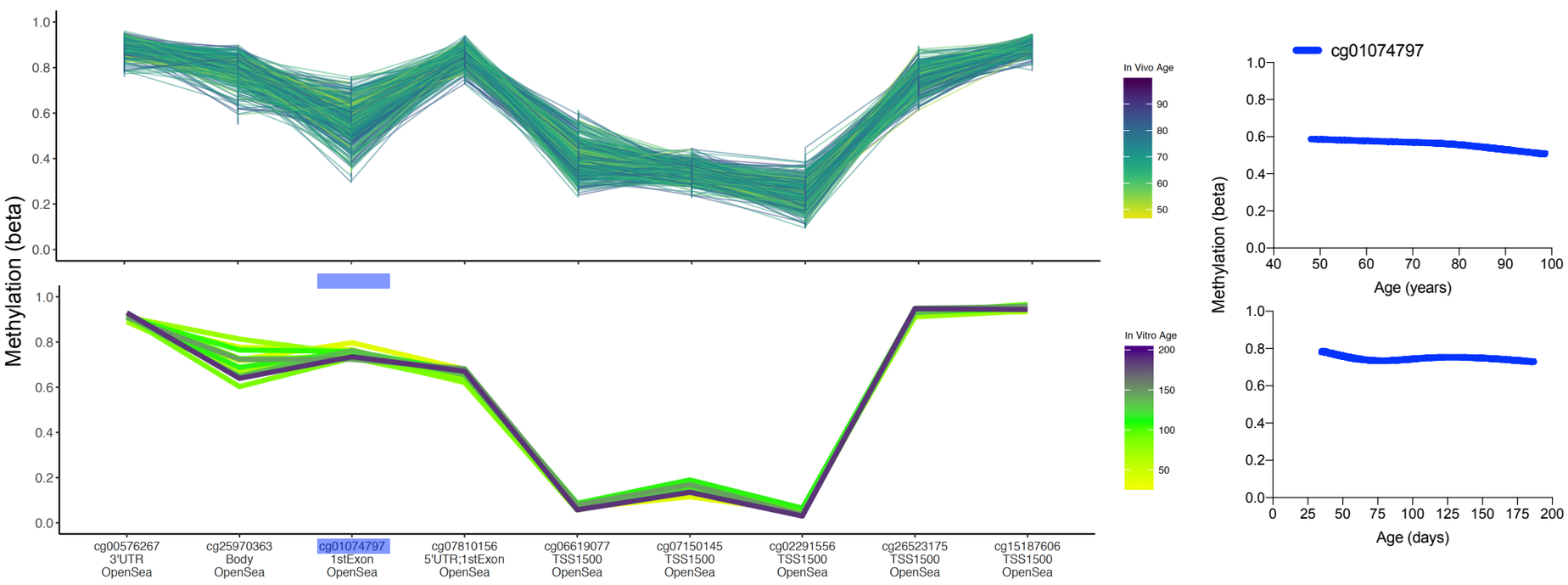

Undetected

CMIP
60th Percentile
GeneCard

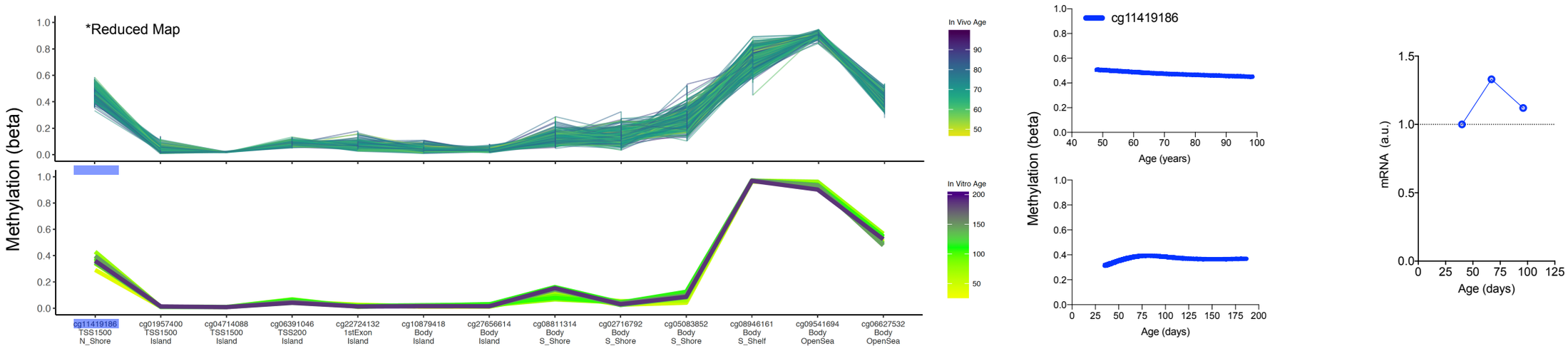

Supplemental Figure S6 - Part 3

Gene

Methylation Topology

Sig. CpG Sites

RNAseq (Cultured Fibroblasts)

TELO2
76th Percentile
GeneCard

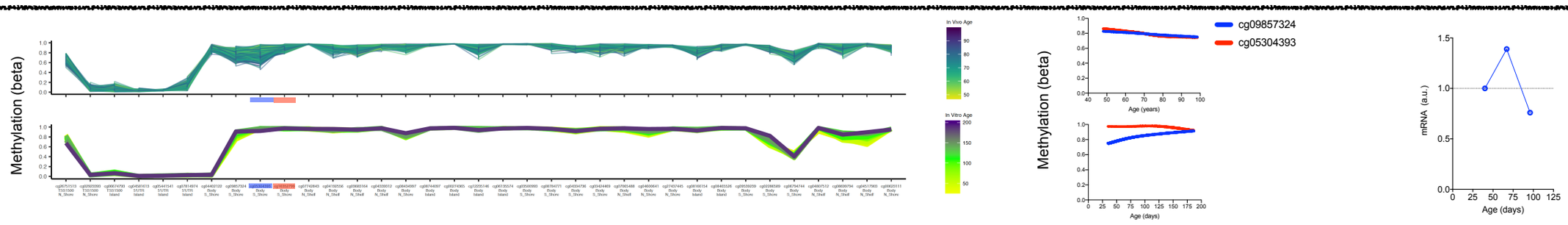

PARP3
89th Percentile
GeneCard

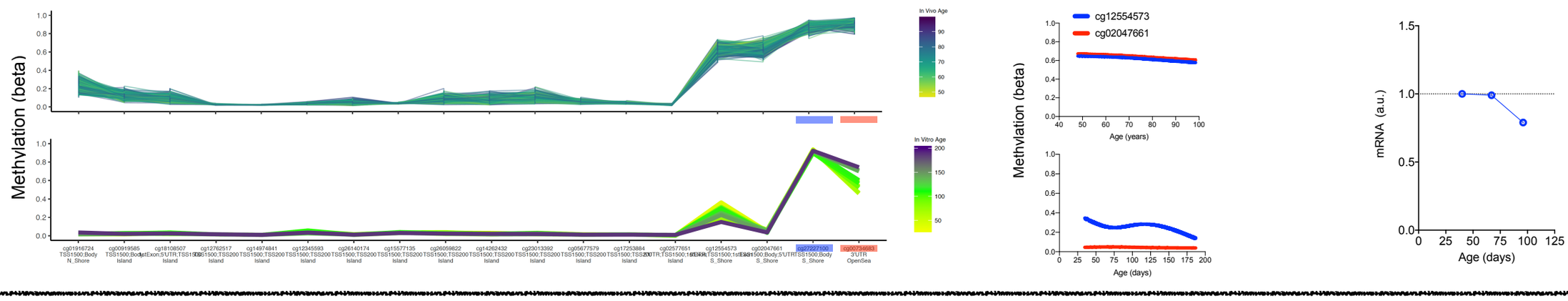

SORBS1
49th Percentile
GeneCard

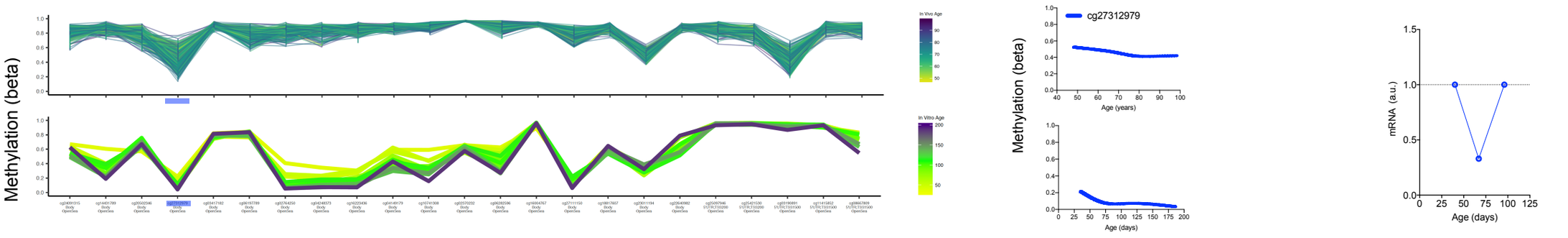

APOL1
58th Percentile
GeneCard

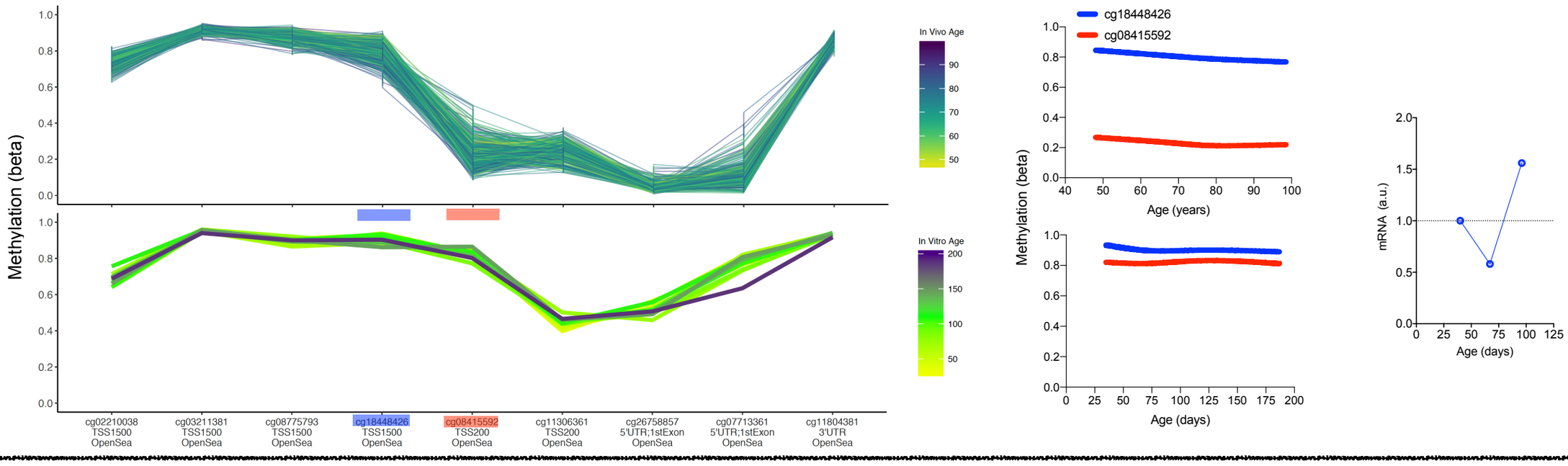

NRG2
20th Percentile
GeneCard

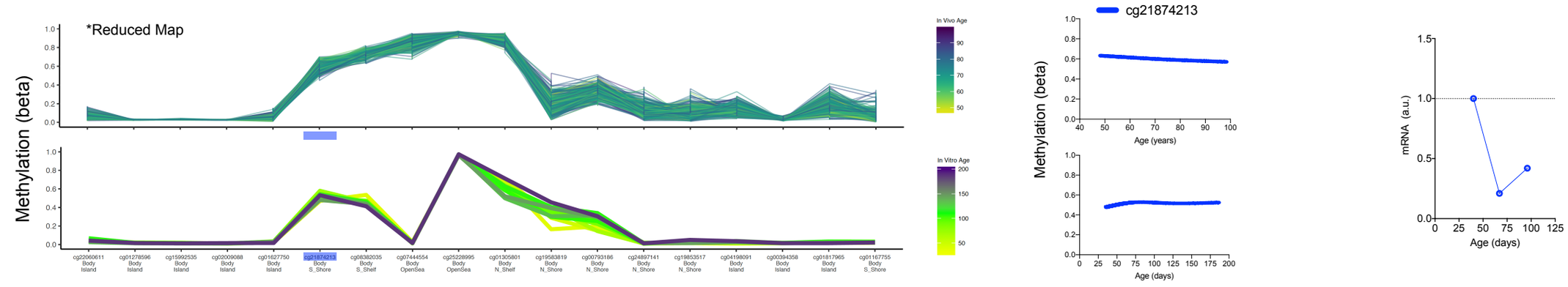

CACNA1G
23rd Percentile
GeneCard

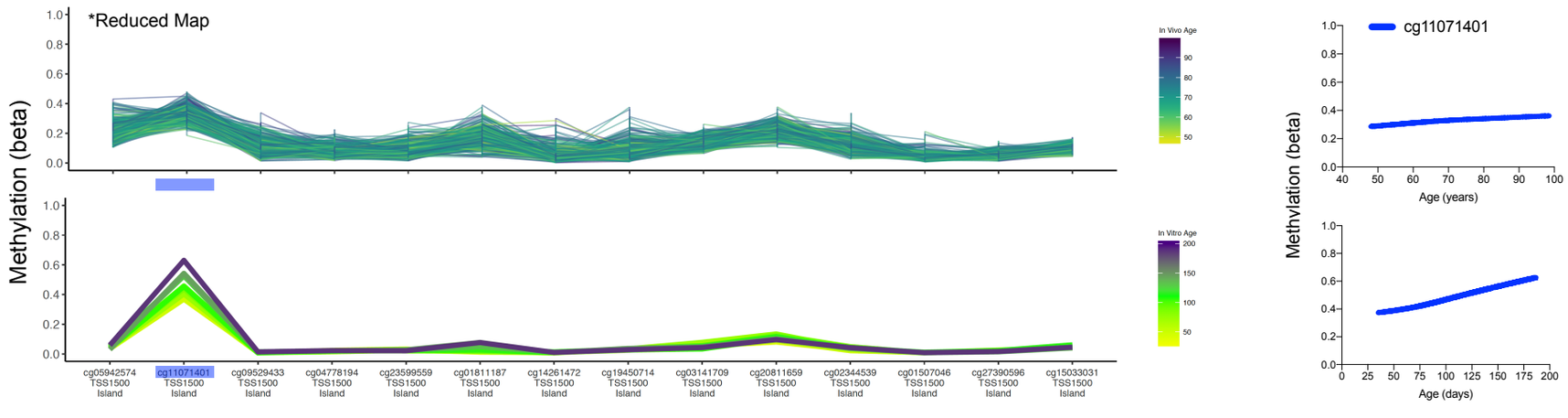

Undetected

Supplemental Figure S6 - Part 4

Supplemental Figure S6 - Part 5

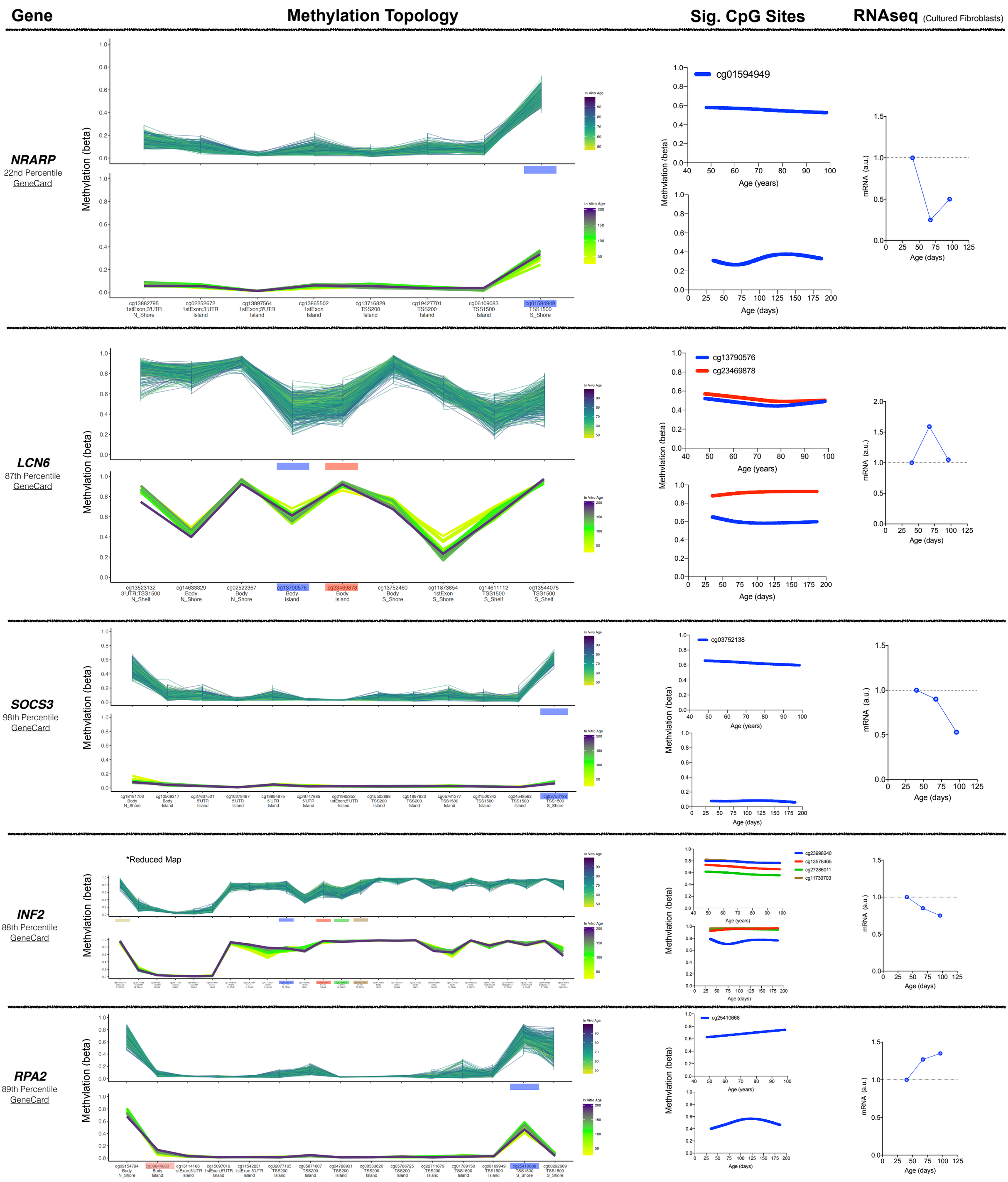

Figure S6. Age-related DNAm gene topology graphs illustrate the degree of conservation between human blood and cultured fibroblasts.

Detailed CpG-by-CpG gene topology maps for all 29 genes reporting at least one significant age-related CpG in the 20-year human blood longitudinal study by Wang et al. (2018). The first gene shown is *ELOVL2* for reference, as in Figure 2. The percentile shown indicates the average transcript level for each gene relative to all other transcript: 1st percentile indicates high expression, 99th percentile indicates low expression.